Electronic Supplementary Material for "Modelling and analysis of bacterial tracks suggest an active reorientation mechanism in *Rhodobacter sphaeroides*"

S1 Depth of microscope field

The total depth of field of an optical microscope is given by [1]

$$d_{\text{tot}} = \frac{\lambda_0 n}{\text{NA}^2} + \frac{ne}{M\,\text{NA}}, \tag{S1}$$

where λ_0 is the wavelength of the illuminating light, n is the refractive index of the immersion oil, NA is the numerical aperture of the objective lens, M is the magnification and e is the lateral resolution (the smallest distance that can be determined in the image plane). In our case, these parameters take the following values: $\lambda_0 \approx 0.5\ \mu$m, $n = 1.5$, NA $= 0.65$, $M = 40$ and $e \approx 0.4\,\mu$m. We therefore compute $d_{\text{tot}} \approx 1.7\,\mu$m.

S2 Derivation of MSD for non-motile bacteria

Integrating equation (3) gives

$$\mathbf{x}(t) = \zeta_t^{-1} \int_0^t \boldsymbol{\xi}(u)\,\mathrm{d}u. \tag{S2}$$

The mean squared displacement (MSD) is defined by

$$\langle \|\mathbf{x}(t)\|^2 \rangle = \zeta_t^{-2} \left\langle \int_0^t \int_0^t \boldsymbol{\xi}(u) \cdot \boldsymbol{\xi}(v)\,\mathrm{d}u\,\mathrm{d}v \right\rangle = 2\zeta_t^{-2} \int_0^t \int_0^t \langle \xi_x(u)\xi_x(v) \rangle\ \mathrm{d}u\,\mathrm{d}v. \tag{S3}$$

The second equality is obtained by noting that the components $\xi_x(t)$, $\xi_y(t)$ of the 2D vector $\boldsymbol{\xi}(t)$ are independent and identically distributed and applying Fubini's theorem [2]. Substituting (2) and integrating, we obtain

$$\langle \|\mathbf{x}(t)\|^2 \rangle = 4\frac{kT}{\zeta_t} t = 4D_t t, \tag{S4}$$

where $D_t = kT/\zeta_t$ is the translational diffusion coefficient. Equation (S4) is identical to results presented in the literature on this subject [3].

S3 Modified censoring method

Figure S1 shows the analogous plots to those in Figure 8 of the main text, computed using the non-chemotactic dataset with the same censoring parameters as used in the original study [4]. The departure from linearity in the MSAC is more significant at shorter timescales than those apparent with the modified censoring process. Even more striking is the departure from normality in the observed distributions of framewise angle changes. This discrepancy is significantly reduced when the modified censoring process is used, suggesting that the 85 additional tracks removed from the non-chemotactic dataset in our modified censoring process are from a distinct subpopulation with greatly altered motility. This is further supported by the appearance of the additional tracks, ten of which are plotted in Figure S2. Comparing Figure S2 with Figure 1 in the main text, we see that these tracks are more tortuous than the majority of tracks in this dataset, which appear smooth and contain no stops. It is likely that these tracks arise from bacteria with damaged motility apparatus, or collections of two or more attached bacteria.

S4 Derivation of observed cell displacement distribution

Starting from equation (6), we may write

$$\mathbf{x}(t) = \zeta_t^{-1} \int_0^t \boldsymbol{\xi}(u)\,\mathrm{d}u = \sqrt{2D_t}\,\mathbf{B}(t), \tag{S5}$$

where $\mathbf{B}(t) = (B_x(t), B_y(t))$ denotes the 2D Wiener process [5], whose components are independent and normally distributed with zero mean and variance t. The multiplicative factors on the right-hand side of (S5) are required to correct for the non-unit variance of the white noise force $\boldsymbol{\xi}(t)$. The characteristic functions of $B_x(t)$, $B_y(t)$ are given by

$$\langle e^{iuB_x(t)} \rangle = \langle e^{iuB_y(t)} \rangle = e^{-u^2 t/2}. \tag{S6}$$

The absolute displacement $R(\tau)$ over a time step $\tau = t - t'$ for $t > t'$ is given by the square root of a sum of squared normal random variables,

$$R(\tau) = \|\mathbf{x}(t) - \mathbf{x}(t')\| = \sqrt{(x(t) - x(t'))^2 + (y(t) - y(t'))^2}. \tag{S7}$$

Since $x(t)$ is normally distributed, so too is the difference, $x(t) - x(t')$, and thus $R(\tau)$ has probability density function (PDF)

$$f_R(r;\tau) = \frac{1}{\sqrt{2D_t\tau}} f_\chi\left(\frac{r}{\sqrt{2D_t\tau}}, 2\right), \tag{S8}$$

where $f_\chi(\cdot, k)$ denotes the PDF of the χ distribution with k degrees of freedom.

S5 Derivation of analytic results for run-only model

We begin our analysis of the run-only model (8)–(10) by deriving expressions for the first and second moments of the orientation angle, $\phi(t)$. Integrating equation (10) subject to the initial condition $\phi(0) = 0$ and using (S5), we obtain

$$\phi(t) = \sqrt{2D_r} B_x(t), \tag{S9}$$

where $D_r = kT/\zeta_r$ denotes the rotational diffusion coefficient. This, rather than ζ_r and T, is the quantity of interest in most experimental studies in this area. Using properties of the Wiener process, we see that the mean orientation angle is simply $\langle\phi(t)\rangle = 0$, while the mean squared angle is given by

$$\langle\phi^2(t)\rangle = 2D_r t. \tag{S10}$$

We now compute the first and second moments of the position vector. Substituting (S9) into (8), integrating subject to $x(0) = 0$ and rewriting the cosine function in complex form yields

$$x(t) = c\int_0^t \left(e^{i\sqrt{2D_r}B(s)} + e^{-i\sqrt{2D_r}B(s)}\right) \mathrm{d}s. \tag{S11}$$

Taking the mean of both sides, applying Fubini's theorem [2], substituting (S6) and integrating, we obtain

$$\langle x(t)\rangle = \frac{c}{D_r}\left(1 - e^{-D_r t}\right). \tag{S12}$$

From (S12) we see that $\langle x(t)\rangle \approx ct$ for small t, indicating that the propulsion of the bacterium initially dominates over rotational diffusion and the motion is approximately ballistic. Over a long timescale, $\langle x(t)\rangle$ tends to the constant ratio c/D_r, indicating that rotational diffusion overrides the effect of the propulsion and that, on average, our model bacterium can only travel a certain distance from its starting point before being constrained by the randomising rotational buffeting. Since we assume that $y(0) = \phi(0) = 0$, by symmetry we have $\langle y(t)\rangle = 0$ for all $t > 0$.

The second moment of $x(t)$ is given by

$$\langle x^2(t)\rangle = c^2\left\langle \int_0^t \cos\left(\sqrt{2D_r}B(u)\right)\mathrm{d}u \int_0^t \cos\left(\sqrt{2D_r}B(v)\right)\mathrm{d}v \right\rangle. \tag{S13}$$

Interchanging the order of integration using Fubini's Theorem and using standard properties of the Wiener process we obtain

$$\langle x^2(t)\rangle = \left(\frac{c}{D_r}\right)^2\left(\frac{2}{3}e^{-D_r t} + \frac{1}{12}e^{-4D_r t} - \frac{3}{4} + D_r t\right). \tag{S14}$$

A similar process may be followed to obtain the second moment in the y-coordinate, which is given by

$$\langle y^2(t)\rangle = \left(\frac{c}{D_r}\right)^2\left(\frac{4}{3}e^{-D_r t} - \frac{1}{12}e^{-4D_r t} - \frac{5}{4} + D_r t\right). \tag{S15}$$

From (S14) and (S15), we see that on a timescale that is short relative to the diffusion coefficient, $t \ll 1/D_r$, we have $\langle x^2(t)\rangle \approx c^2t^2$ and $\langle y^2(t)\rangle \approx c^2t^2/2$, which again indicates that movement is ballistic. This is also the case for the VJ process over short timescales [6]. For longer times $t \gg 1/D_r$, both second moments vary approximately as c^2t/D_r. This asymptotically linear behaviour of the second moment is characteristic of a diffusive process and is again similar to that observed in the VJ process. Coupling this result with equation (S12), we see that the mean position of the bacterium reaches an asymptotic value, but the bacterium continues to explore its environment in a diffusive manner. Furthermore, we may combine these equations to obtain

an expression for the standard deviations of $x(t)$ and $y(t)$ using the standard result

$$\mathrm{std}(x(t)) = \sqrt{\langle x^2(t)\rangle - \langle x(t)\rangle^2}. \tag{S16}$$

We obtain

$$\mathrm{std}(x(t)) = \frac{c}{D_r}\left(\frac{1}{12}e^{-4D_rt} - e^{-2D_rt} + \frac{8}{3}e^{-D_rt} + D_rt - \frac{7}{4}\right)^{1/2}, \tag{S17}$$

$$\mathrm{std}(y(t)) = \frac{c}{D_r}\left(-\frac{1}{12}e^{-4D_rt} + \frac{4}{3}e^{-D_rt} + D_rt - \frac{5}{4}\right)^{1/2}. \tag{S18}$$

S6 Derivation of analytic results for run-and-stop model

We begin our analysis of the run-and-stop model (11)–(13) by noting that the solution to equation (13) matches that of (10). We now consider the stochastic switching force $F(t)$ in equations (11)–(12). Let $p(t;s) = \mathbb{P}(F(t) = 1|F(s) = 1)$ denote the probability that the bacterium is running at time t, given that it is running at time $s < t$. The evolution of $p(t;s)$ is governed by the forward equation [7]

$$\frac{\mathrm{d}p}{\mathrm{d}t} = \lambda_r - (\lambda_r + \lambda_s)p, \tag{S19}$$

subject to $p(s;s) = 1$, hence we have

$$p(t;s) = \frac{1}{\lambda_s + \lambda_r}(\lambda_r + \lambda_s e^{-(\lambda_s+\lambda_r)(t-s)}). \tag{S20}$$

Since $F = 1$ is the only allowable non-zero value, the ensemble average of $F(t)$ is given by

$$\langle F(t)\rangle = p(t;0) = \frac{1}{\lambda_s + \lambda_r}(\lambda_r + \lambda_s e^{-(\lambda_s+\lambda_r)t}), \tag{S21}$$

and its autocorrelation function is given by [8]

$$\langle F(s)F(t)\rangle = \langle F(t)|F(s) = 1\rangle\langle F(s)\rangle \tag{S22}$$

$$= p(t;s)p(s;0) \tag{S23}$$

$$= \left(\frac{1}{\lambda_s + \lambda_r}\right)^2 \left(\lambda_r + \lambda_s e^{-(\lambda_s+\lambda_r)(t-s)}\right)\left(\lambda_r + \lambda_s e^{-(\lambda_s+\lambda_r)s}\right), \tag{S24}$$

for $0 \leq s \leq t$. Integrating (11) gives

$$x(t) = c \int_0^t F(s) \cos\left(\sqrt{2D_r} B(s)\right) \mathrm{d}s. \tag{S25}$$

Noting the independence of $F(t)$ and $B(t)$, we carry out similar manipulations to those used in deriving (S12) to show that the ensemble average of $x(t)$ is given by

$$\langle x(t) \rangle = \frac{c}{\lambda_s + \lambda_r} \left[\frac{\lambda_r}{D_r} (1 - e^{-D_r t}) + \frac{\lambda_s}{D_r + \lambda_s + \lambda_r} (1 - e^{-(D_r + \lambda_s + \lambda_r)t}) \right]. \tag{S26}$$

As for the run-only model, we have $\langle y(t) \rangle = 0$ by symmetry. The second moment of $x(t)$ is given by

$$\langle x^2(t) \rangle = c^2 \int_0^t \int_0^t \langle F(u)F(v) \rangle \left(\left\langle \cos\left[\sqrt{2D_r}(B(v) + B(u)) \right] \right\rangle + \left\langle \cos\left[\sqrt{2D_r}(B(v) - B(u)) \right] \right\rangle \right) \mathrm{d}u \, \mathrm{d}v. \tag{S27}$$

Substituting equation (S24) into (S27) and using standard properties of the Wiener process gives

$$\langle x^2(t) \rangle = \left(\frac{c\lambda_r}{\lambda_s + \lambda_r} \right)^2 \int_0^t \int_0^v \left(e^{-D_r(3u+v)} + e^{-D_r(v-u)} \right) \left(1 + \frac{\lambda_s}{\lambda_r} e^{-(\lambda_s + \lambda_r)u} \right) \left(1 + \frac{\lambda_s}{\lambda_r} e^{-(\lambda_s + \lambda_r)(v-u)} \right) \mathrm{d}u \, \mathrm{d}v. \tag{S28}$$

The integral in equation (S28) is straightforward to calculate but is not presented here for the sake of brevity. A similar expression may be derived for the second moment of $y(t)$, and is given by

$$\langle y^2(t) \rangle = \left(\frac{c\lambda_r}{\lambda_s + \lambda_r} \right)^2 \int_0^t \int_0^v \left(e^{-D_r(v-u)} - e^{-D_r(3u+v)} \right) \left(1 + \frac{\lambda_s}{\lambda_r} e^{-(\lambda_s + \lambda_r)u} \right) \left(1 + \frac{\lambda_s}{\lambda_r} e^{-(\lambda_s + \lambda_r)(v-u)} \right) \mathrm{d}u \, \mathrm{d}v. \tag{S29}$$

Expressions for the standard deviations of $x(t)$ and $y(t)$ may be then be computed from (S28) and (S29).

In the case of the run-and-active-stop model, the moments can be derived using similar steps to those shown above. However, we do not solve for the moments of this model here as the result would be algebraically cumbersome and not instructive for our purposes.

References

1. Hecht, E.. Optics. 4 ed.; Addison-Wesley; 2002. ISBN 9780321188786.
2. Priestley, H.. Introduction to Integration. Oxford University Press; 1997. ISBN 0198501242.
3. Berg, H.. Random Walks in Biology. Princeton University Press; 1993. ISBN 0691000646.
4. Rosser, G., Fletcher, A., Wilkinson, D., de Beyer, J., Yates, C., Armitage, J., et al. Novel methods for analysing bacterial tracks reveal persistence in *Rhodobacter sphaeroides*. PLOS Comput Biol 2013;9:e1003276.
5. Klebaner, F.. Introduction to Stochastic Calculus with Applications. World Scientific Publishing Company; 1999. ISBN 186094129X.
6. Othmer, H., Dunbar, S., Alt, W.. Models of dispersal in biological systems. J Math Biol 1988;26:263–298.
7. Grimmett, G., Stirzaker, D.. Probability and Random Processes. 3rd ed.; Oxford University Press, USA; 2001. ISBN 0198572220.
8. Gardiner, C.. Handbook of Stochastic Methods: For Physics, Chemistry and the Natural Sciences. 3rd ed.; Springer; 2004. ISBN 3540208828.

S7 Supplementary Figures

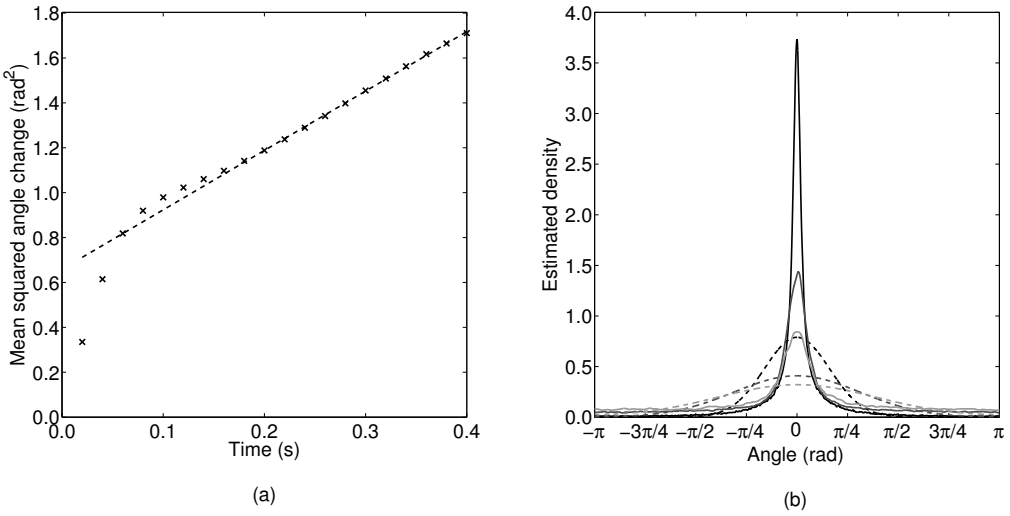

Figure S1. Extracting characteristics of noise from the *R. sphaeroides* non-chemotactic dataset obtained by Rosser et al. [4] with no modification to the censoring process. (a) The observed MSAC (black crosses) with linear fit (dashed line). The slope of the fit is $0.255\,\mathrm{rad}^2\,\mathrm{s}^{-1}$. (b) The estimated PDF of angle changes (solid line), overlaid with the wrapped normal distribution with variance computed from the data (dashed line). The three shades denote different values for the sampling interval, τ. Black: $\tau = 0.02$ s; dark grey: $\tau = 0.1$ s; light grey: $\tau = 0.2$ s.

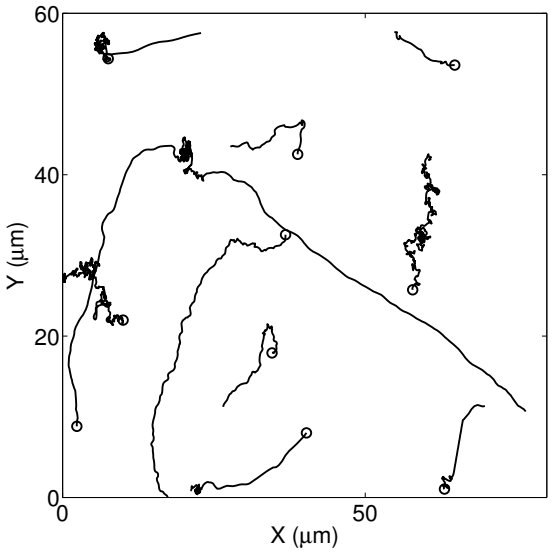

Figure S2. Ten randomly-selected tracks from the non-chemotactic dataset that are included in the original study [4] but excluded with the modified censoring process used here.

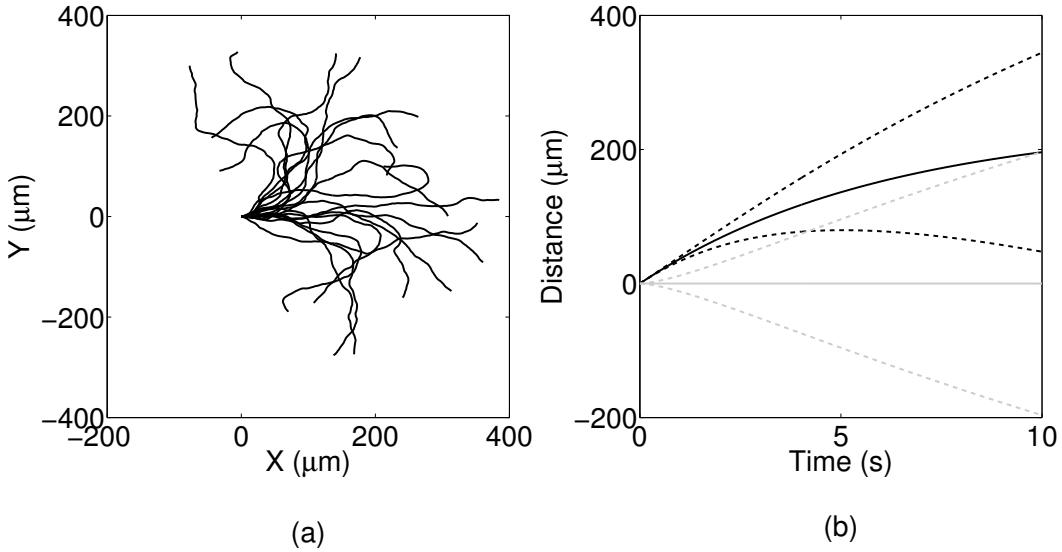

Figure S3. (a) 20 sample trajectories generating by simulating the run-only model (8)–(10). (b) Mean (solid line) and mean ± standard deviation (dashed lines) for x (black) and y (grey) position of a particle in the run-only model.

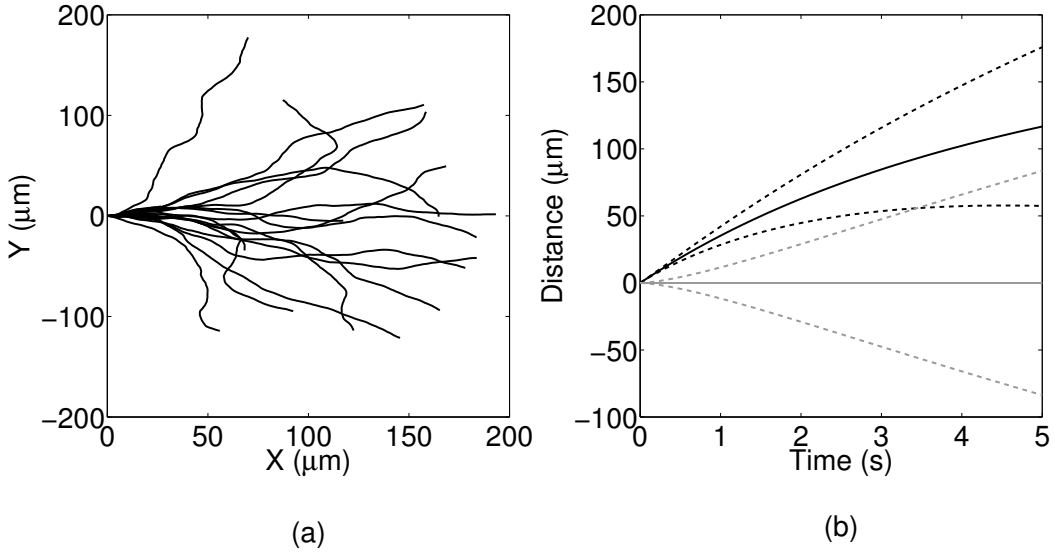

Figure S4. (a) 20 sample trajectories computed by solving the run-and-stop model (11)–(13). (b) Mean (solid line) and mean ± standard deviation (dashed lines) for x (black) and y (grey) coordinates of a particle in the run-and-stop model.

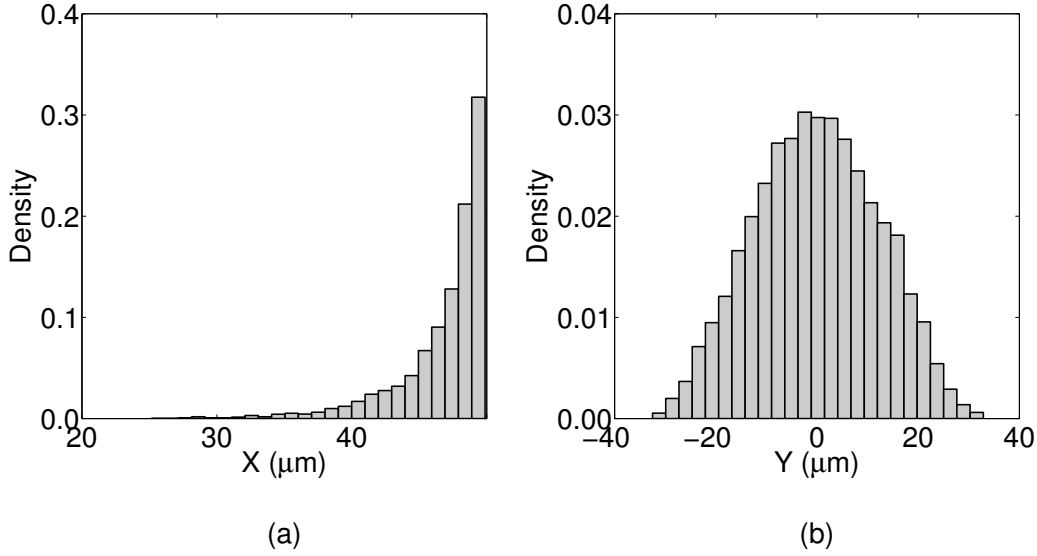

Figure S5. Histograms of the x and y position of simulated particles in the run-only model (8)–(10) with sampling time step $\tau = 1$ s.